

**Internuclear distance and effects of Born–Oppenheimer breakdown for PtS, determined from its pure rotational spectrum**

Stephen A. Cooke and Michael C. L. Gerry

Citation: *The Journal of Chemical Physics* **121**, 3486 (2004); doi: 10.1063/1.1769365

View online: <http://dx.doi.org/10.1063/1.1769365>

View Table of Contents: <http://scitation.aip.org/content/aip/journal/jcp/121/8?ver=pdfcov>

Published by the [AIP Publishing](#)

---

**Articles you may be interested in**

Rotational spectra of rare isotopic species of fluoriodomethane: Determination of the equilibrium structure from rotational spectroscopy and quantum-chemical calculations

*J. Chem. Phys.* **137**, 024310 (2012); 10.1063/1.4731284

The rotational spectrum of  $\text{CuCCH} (\tilde{X} \Sigma^+)$ : A Fourier transform microwave discharge assisted laser ablation spectroscopy and millimeter/submillimeter study

*J. Chem. Phys.* **133**, 174301 (2010); 10.1063/1.3493690

An investigation of the molecular geometry and electronic structure of nitril chloride by a combination of rotational spectroscopy and ab initio calculations

*J. Chem. Phys.* **128**, 204305 (2008); 10.1063/1.2920487

Fourier transform microwave spectroscopy and Fourier transform microwave–millimeter wave double resonance spectroscopy of the ClOO radical

*J. Chem. Phys.* **121**, 8351 (2004); 10.1063/1.1792591

Investigation of the pure rotational spectrum of magnesium monobromide by Fourier transform microwave spectroscopy

*J. Chem. Phys.* **107**, 9835 (1997); 10.1063/1.475280

---



# Internuclear distance and effects of Born–Oppenheimer breakdown for PtS, determined from its pure rotational spectrum

Stephen A. Cooke and Michael C. L. Gerry<sup>a)</sup>

*Department of Chemistry, University of British Columbia, 2036 Main Mall, Vancouver, B.C. V6T 1Z1, Canada*

(Received 12 March 2004; accepted 17 May 2004)

Platinum monosulfide PtS has been prepared in its  $X0^+$  ground electronic state by laser ablation of Pt in the presence of  $H_2S$ . The rotational spectra of eight isotopic species have been measured with a cavity pulsed jet Fourier-transform microwave spectrometer. Spectral analysis using a multi-isotopomer Dunham-type expression produced values for  $Y_{01}$ ,  $Y_{02}$ ,  $Y_{11}$ , and  $Y_{21}$ , along with large values for Born–Oppenheimer breakdown (BOB) parameters for both atoms of the molecule. The BOB parameters are rationalized in terms of the molecular electronic structure and nuclear field shift effects. A large negative  $^{195}\text{Pt}$  nuclear spin-rotation constant has been rationalized in terms of the electron-nucleus dipole-dipole hyperfine constant. The equilibrium bond length in the Born–Oppenheimer approximation has been evaluated. © 2004 American Institute of Physics. [DOI: 10.1063/1.1769365]

## I. INTRODUCTION

Although it is now over 70 years since Dunham first published his model for the energy levels of diatomic molecules,<sup>1</sup> this model continues to provide the basis for the analysis of their high resolution spectra. However, because of the precision and accuracy of spectroscopic measurements, it has had to be modified to incorporate effects of Born–Oppenheimer breakdown (BOB). The basic procedure for doing this for  $X^1\Sigma^+$  molecules was published over 20 years ago by Watson<sup>2,3</sup> and Bunker.<sup>4,5</sup> This takes into account both adiabatic and nonadiabatic effects but neglects possible effects due to the “finite size of the nuclei, the second-order contribution of spin-orbit coupling, and other relativistic effects.”<sup>2</sup> This approach was expected, and found, to be necessary for the analysis of spectra of light diatomic molecules.<sup>2</sup> A different formalism of Watson’s model has been developed by LeRoy.<sup>6</sup>

Anomalies in the analysis of the millimeter wave spectra of the lead chalcogenides and thallium halides prompted Tiemann *et al.* to include effects from the finite sizes of the nuclei.<sup>7–9</sup> Initial spectral analysis produced apparent large adiabatic BOB terms for the metals. However, further study showed that the anomalies arose because these nuclei had a finite charge distribution. They were accounted for with a revision of Watson’s formula which included new “field-shift” parameters.<sup>8</sup>

In rotational spectroscopy effects of BOB have appeared mostly in millimeter wave spectra, whose measurements have always carried many significant figures. However, measurements using cavity pulsed jet Fourier-transform microwave (FTMW) spectrometers are now so precise that BOB terms have been determined from spectra measured at much lower frequencies, even for molecules containing heavy atoms. For example, they have been needed in recent analyses

of spectra of ZrO and ZrS (Ref. 10), HfO (Ref. 11), HfS (Ref. 12), PtSi (Ref. 13), and BiN (Ref. 14). All these molecules have relatively large BOB terms, with the last two showing field-shift effects for Pt and Bi, respectively.

In the recent example of PtSi (Ref. 13) initial analyses omitting field-shift terms showed a significant difference in magnitude between the respective Watson-type BOB parameters ( $\Delta_{01}^{\text{Pt}}$  and  $\Delta_{01}^{\text{Si}}$ ). The differences were surmised to be due to field-shift effects for Pt. Fits to the experimental data alone could not, however, separate adiabatic and nonadiabatic effects from field-shift effects because of high correlations. Because adiabatic and nonadiabatic contributions are usually approximately the same for the two nuclei in a diatomic molecule, the field-shift parameters could be estimated by assuming this to be the case in PtSi and refitting the data to the Pt field-shift parameter and one  $\Delta_{01}$  parameter. Reasonable values for both were seemingly obtained. However, since it was found that the field-shift parameter was large in magnitude and of opposite sign to those found for the Pb-chalcogenides and Tl-halides it was necessary to verify it independently.

Schlembach and Tiemann<sup>8</sup> showed that the field-shift parameter  $V_{01}^A$  for atom A is proportional to  $(d\rho_{e1}/dr)_{r_e}^A$ , the derivative of the electron density at nucleus A with respect to the internuclear distance, evaluated at the equilibrium distance. In their early (1982) work they estimated values for Pb and Tl using Hartree–Fock evaluations. Since that time, this parameter has fallen into disuse. This is unfortunate, because it can provide helpful information, verifiable experimentally, about molecular electronic structures. Accordingly we have recently demonstrated that density functional theory (DFT) may be used to estimate field-shift parameters.<sup>15</sup> Application to PtSi verified that the experimental field-shift parameter is indeed reasonable.<sup>13</sup>

The present paper extends this work to platinum monosulfide PtS. This molecule has, however, rather different

<sup>a)</sup>Electronic mail: mgerry@chem.ubc.ca

properties from those previously reported. In a Hund's case (a) or (b) coupling scheme its electronic ground state would be  $X^3\Sigma^-$ . However, case (c) coupling actually applies, with a large spin-orbit coupling, and the ground state is  $X^0^+$ .<sup>16</sup> Many bands have the appearance of  $^1\Sigma - ^1\Sigma$  transitions, and the ground state could easily be assigned as  $X^1\Sigma^+$ . The same phenomenon is found for isoelectronic PtO,<sup>17,18</sup> for which the ground state was indeed initially thought to be  $^1\Sigma^+$ .

In conjunction with the electronic spectrum, Li *et al.*<sup>16</sup> used pump-probe microwave-optical double resonance (MODR) to record the  $J=5-4$ ,  $6-5$ , and  $8-7$  pure rotational transitions of the three most abundant isotopomers of PtS. The resolution, although high, was insufficient for measurement of  $^{195}\text{Pt}$  hyperfine structure. The dataset included only vibrational ground state transitions, and thus precluded a Dunham-type analysis. The dipole moment of PtS has also been measured.<sup>19</sup>

In the present work the MODR measurements have been extended by FTMW spectroscopy to further  $J$  values and isotopomers in several vibrational states, at considerably higher resolution. Unusual  $^{195}\text{Pt}$  spin-rotation coupling has been found. The results could be treated with the same Dunham-type analysis as is used for closed shell molecules. The large BOB terms found are rationalized in terms of electronic structure, and the internuclear distance has been evaluated.

## II. EXPERIMENTAL AND CALCULATION METHODS

### A. Spectroscopic measurements

A pulsed Nd:YAG laser beam of wavelength 1064 nm was focused onto a rotating glass rod wrapped with platinum foil. The rod and foil were mounted in an ablation system specially designed for our FTMW spectrometer.<sup>20</sup> The resulting ablation produced a plasma of Pt, which then reacted with a small amount ( $\sim 0.1\%$ ) of  $\text{H}_2\text{S}$  (Matheson  $\geq 99\%$  purity) contained in Ar. This gas mixture was issued from a reservoir held at high pressure (5–7 atm) via a solenoid valve (series 9, General Valve). The reaction mixture then underwent a supersonic expansion into an evacuated Fabry–Perot cavity of a Balle–Flygare type<sup>21</sup> Fourier-transform microwave (FTMW) spectrometer.<sup>22</sup> The microwave spectrum of PtS was recorded between 8 and 18 GHz. The gas expansion occurred parallel to the central axis of the cavity mirrors, and parallel to the direction of propagation of the microwaves, with the result that all transitions were observed as Doppler doublets. Linewidths with this arrangement were typically 7–10 kHz (FWHM). Frequency measurements were referenced to a Loran frequency standard accurate to 1 part in  $10^{10}$ ; reported line frequencies are estimated to be accurate to better than  $\pm 1$  kHz.

### B. Theoretical calculations

Density functional theory (DFT) calculations following the procedure outlined by Cooke *et al.*<sup>15</sup> were used to predict the field-shift parameters  $V_{01}^{\text{Pt}}$  and  $V_{01}^{\text{S}}$ . The calculation determined the derivative of the electron density at the given nucleus with respect to the internuclear distance, and the field shift parameter for Pt was estimated using

$$V_{01}^{\text{Pt}} = \frac{Z_{\text{Pt}} e^2}{3 \epsilon_0 k_e r_e} \left( \frac{d\rho_{el}}{dr} \right)_{r_e}^{\text{Pt}} \quad (1)$$

with an analogous equation for  $V_{01}^{\text{S}}$ .  $Z_{\text{Pt}}$  is the atomic number for Pt,  $e$  is the elementary charge,  $\epsilon_0$  is the permittivity of free space,  $k_e$  is the harmonic force constant,  $\rho_{el}$  is the electron density, and  $r_e$  is the equilibrium internuclear distance.

The DFT calculation was performed using the Amsterdam density functional program<sup>23</sup> (ADF) and used an all-electron basis set (QZ4P) of Slater-type orbitals (in preference to Gaussian-type orbitals because the former have better cusp behavior). Attempts to account for relativistic effects were made using the zeroth-order regular approximation (ZORA).<sup>24,25</sup> Use was also made of the statistical average of orbital potentials (SAOP) model.<sup>26</sup> Single point calculations giving the electron densities,  $\rho_{el}$ , at a series of different internuclear distances were carried out. A polynomial was then fitted to the derived densities and its derivative gave the required quantity. These calculations also produced a potential energy curve for PtS, from which an equilibrium internuclear distance and other spectroscopic parameters could be predicted.

## III. RESULTS AND ANALYSIS

### A. Spectra and assignments

The spectroscopic constants in Ref. 16 were used to predict the corresponding transitions for those isotopomers in the frequency range of our FTMW spectrometer. Lines requiring the presence of both Pt and  $\text{H}_2\text{S}$  in the reaction mixture were quickly found at the predicted frequencies. Some searching then revealed transitions of previously unobserved isotopomers and of vibrationally excited molecules. The assignments were confirmed by the isotopic distribution of the lines and by the hyperfine structures of the transitions containing  $^{195}\text{Pt}$  ( $I=1/2$ ).

The frequencies of the measured transitions are given with their assignments in Table I. The measurements of Ref. 16 are included for completeness.

For the isotopomers containing  $^{195}\text{Pt}$  the coupling scheme  $\mathbf{J}+\mathbf{I}=\mathbf{F}$  has been employed. The  $J=1-0$  transition of  $^{195}\text{Pt}^{32}\text{S}$  is illustrated in Fig. 1.

### B. $^{195}\text{Pt}$ hyperfine analysis

Because the program used to perform the Dunham-type fits described below does not include hyperfine structure, preliminary analyses were carried out for isotopic species containing  $^{195}\text{Pt}$ . Their line frequencies were fit to the constants in the Hamiltonian,

$$\mathbf{H} = B_v \mathbf{J}^2 - D_v \mathbf{J}^4 + C_I \mathbf{I} \cdot \mathbf{J} \quad (2)$$

using Pickett's least-squares fitting program SPFIT.<sup>27</sup> Each vibrational state was treated separately, giving its rotational constant  $B_v$ , centrifugal distortion constant  $D_v$ , and  $^{195}\text{Pt}$  nuclear spin-rotation constant  $C_I$ . The fits were to the data in Table I. The resulting constants are in Table II, in comparison with those previously reported for PtSi and PtCO.

It will be noted that  $C_I$  for PtS is much bigger in magnitude than and of opposite sign to the values for the other two molecules. Using the constants given in Table II the

TABLE I. Measured transition frequencies for PtS.

Isotopomer	$J' - J''$	$F' - F''$	$v$	Frequency (MHz)	Obs. - calc. (kHz) <sup>a</sup>
<sup>192</sup> Pt <sup>32</sup> S	1-0		0	8844.1512	0.4
<sup>194</sup> Pt <sup>32</sup> S	1-0		0	8831.1458	-0.2
	2-1		0	17 662.2578	0.6
	5-4		0	44 155.0373	3.1 <sup>b</sup>
	6-5		0	52 985.6640	5.6 <sup>b</sup>
	8-7		0	70 646.2476	1.7 <sup>b</sup>
	1-0		1	8792.9563	0.0
	2-1		1	17 585.8765	-1.3
	1-0		2	8754.6948	-0.2
	2-1		2	17 509.3554	0.2
	<sup>195</sup> Pt <sup>32</sup> S	1-0	$\frac{1}{2} - \frac{1}{2}$	0	8824.8020
1-0		$\frac{3}{2} - \frac{1}{2}$	0	8824.7016	-0.1 <sup>c</sup>
2-1		$\frac{3}{2} - \frac{1}{2}$	0	17 649.4689	-0.1 <sup>c</sup>
2-1		$\frac{5}{2} - \frac{3}{2}$	0	17 649.4024	0.1 <sup>c</sup>
5-4		d	0	44 122.9370	-47.5 <sup>d</sup>
6-5		d	0	52 947.1850	-16.4 <sup>d</sup>
8-7		d	0	70 594.9310	-47.6 <sup>d</sup>
1-0		$\frac{1}{2} - \frac{1}{2}$	1	8786.6521	0.2 <sup>c</sup>
1-0		$\frac{3}{2} - \frac{1}{2}$	1	8786.5543	-0.2 <sup>c</sup>
2-1		$\frac{3}{2} - \frac{1}{2}$	1	17 573.1726	-0.2 <sup>c</sup>
2-1		$\frac{5}{2} - \frac{3}{2}$	1	17 573.1060	0.2 <sup>c</sup>
1-0		$\frac{1}{2} - \frac{1}{2}$	2	8748.4319	0.0 <sup>c</sup>
1-0		$\frac{3}{2} - \frac{1}{2}$	2	8748.3342	0.0 <sup>c</sup>
<sup>196</sup> Pt <sup>32</sup> S		1-0		0	8818.4021
	2-1		0	17 636.7694	0.4
	5-4		0	44 091.3090	6.7 <sup>b</sup>
	6-5		0	52 909.1940	3.3 <sup>b</sup>
	8-7		0	70 544.3010	0.6 <sup>b</sup>
	1-0		1	8780.2948	-0.3
	2-1		1	17 560.5553	-0.1
	1-0		2	8742.1168	0.0
<sup>198</sup> Pt <sup>32</sup> S	1-0		0	8805.9112	-0.1
	2-1		0	17 611.7885	0.4
	1-0		1	8767.8854	-0.3
	2-1		1	17 535.7367	0.0
<sup>194</sup> Pt <sup>34</sup> S	1-0		0	8386.6878	-0.1
	2-1		0	16 733.3445	-1.7
	1-0		0	8351.3578	4.3
<sup>195</sup> Pt <sup>34</sup> S	1-0	$\frac{1}{2} - \frac{1}{2}$	0	8380.3413	0.0 <sup>c</sup>
	1-0	$\frac{3}{2} - \frac{1}{2}$	0	8380.2445	0.0 <sup>c</sup>
<sup>196</sup> Pt <sup>34</sup> S	1-0		0	8373.9421	-0.2

<sup>a</sup>Apart from <sup>195</sup>PtS these are the observed frequencies minus those calculated from the fitted constants of Table III. See also footnote c below.

<sup>b</sup>These line frequencies were taken from Ref. 16 and given a 100-fold lower weight than the other lines in the fitting procedure.

<sup>c</sup>These data were least-squares fit using the SPFIT program. The obs. - calc. values are the observed frequencies minus those calculated with the constants in Table II.

<sup>d</sup>Taken from Ref. 16. Magnetic hyperfine splitting was not observed for these transitions because of the resolution of the experimental method. In the present work these lines were excluded from the fitting procedures. The obs. - calc. values are the observed frequencies minus the hypothetical line centers obtained from the constants in Table II.

hyperfine splitting in the MODR data of Ref. 16 was calculated. For the  $J=8-7$  transition for example the splitting is predicted to be  $\approx 60$  kHz which is approximately half the line widths obtained in the experiment. This would explain why these splittings were not reported in Ref. 16.

For the Dunham-type analysis hypothetical unsplit frequencies for the well resolved  $J=1-0$  and  $J=2-1$  rotational transitions were calculated from the rotational constants and distortion constants in Table II. Again each isotopomer and

vibrational state were treated separately. Enough significant figures in the constants were retained to ensure that the calculated frequencies were accurate to the experimental uncertainties.

### C. Dunham-type analysis

A general treatment of the rotational energy and fine structure of a diatomic molecule following Hund's case (c)

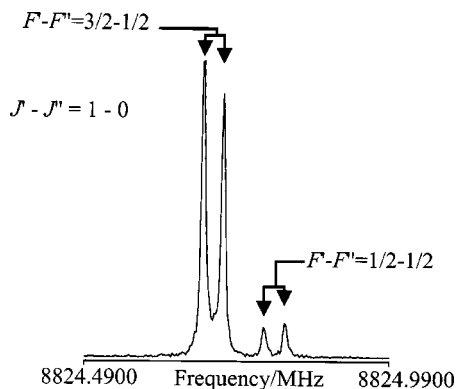


FIG. 1. Power spectrum of the  $J=1-0$  transition of  $^{195}\text{Pt}^{32}\text{S}$ , showing  $^{195}\text{Pt}$  hyperfine structure. 500 averaging cycles.  $4k$  data points were recorded, and the power spectrum is shown as a  $4k$  transformation.

was published by Veseth.<sup>29,30</sup> For a  $^3\Sigma$  state there are three states for each value of  $J$ , one having  $\Omega=0$  and two of opposite parity having  $|\Omega|=1$ . The  $\Omega=0$  and  $|\Omega|=1$  states of the same parity interact through a perturbation operator,

$$\hat{H}_p = -2B\mathbf{J}\cdot\mathbf{J}_a, \quad (3)$$

where  $B$  is the rotational constant,  $\mathbf{J}$  is the operator for the total angular momentum exclusive of nuclear spin, and  $\mathbf{J}_a = \mathbf{L} + \mathbf{S}$ . Here  $\mathbf{L}$  and  $\mathbf{S}$  are the electronic orbital and spin angular momentum operators, respectively. If the interacting vibronic levels having  $\Omega=0$  and  $|\Omega|=1$  are well separated, then Kuijpers, Törring, and Dymanus<sup>31</sup> showed that the rotational energy can be written as

$$E = \left( B - \frac{2P^2}{T_1 - T_0} \right) J(J+1) - \left( D - \frac{8D}{B} \frac{P^2}{T_1 - T_0} \right) \times J^2(J+1)^2 + \dots \quad (4)$$

In this expression,

$$B = (Y_{01} + \epsilon) + Y_{11}(v + \frac{1}{2}) + Y_{12}(v + \frac{1}{2})^2 + \dots, \quad (5)$$

$$D = -Y_{02} - Y_{12}(v + \frac{1}{2}) - Y_{22}(v + \frac{1}{2})^2 + \dots, \quad (6)$$

$$P = \langle v, J_a, \Omega = 1 | B(\mathbf{J}_a) | v', J_a, \Omega = 0 \rangle. \quad (7)$$

In these expressions  $Y_{kl}$  are the Dunham coefficients,  $\epsilon$  is the Dunham correction to  $Y_{01}$ ,  $v$  is a vibrational quantum num-

ber, and  $(T_1 - T_0)$  is the energy difference between the  $|\Omega|=1$  and  $\Omega=0$  states. Eqs. (4)–(7) can be reorganized, to the precision available experimentally, as

$$E = \left[ Y_{01} \left( 1 + \frac{\epsilon}{Y_{01}} - \frac{2P^2}{Y_{01}(T_1 - T_0)} \right) + Y_{11} \left( v + \frac{1}{2} \right) + Y_{21} \left( v + \frac{1}{2} \right)^2 + \dots \right] J(J+1) + \left[ Y_{02} + Y_{12} \left( v + \frac{1}{2} \right) + \dots \right] J^2(J+1)^2 + \dots \quad (8)$$

In Eqs. (7) and (8) the effect of  $P$  is Born–Oppenheimer breakdown, so that the term  $2P^2/Y_{01}(T_1 - T_0)$  gives a measure of this breakdown. Kuijpers, Törring, and Dymanus<sup>31</sup> also pointed out that when this term is very small the usual expressions for a  $X^1\Sigma^+$  molecule apply, and the physical meanings of the  $Y_{kl}$  are well defined.

Equation (8) should thus be compared with Watson's<sup>2,3</sup> expression for the rotational energy of a  $^1\Sigma^+$  molecule  $AB$  (see also Schlembach and Tiemann, Ref. 8),

$$E = \sum_{k,l} Y_{kl} \left( v + \frac{1}{2} \right)^k J^l(J+1)^l \quad (9)$$

with

$$Y_{kl} = \frac{U_{kl}}{\mu^{(k+2l)/2}} \left[ 1 + \frac{m_e}{M_A} \Delta_{kl}^A + \frac{m_e}{M_B} \Delta_{kl}^B \right], \quad (10)$$

where the  $U_{kl}$  are mass-independent Dunham parameters,  $\mu$  is the reduced mass of the molecule ( $=M_A M_B / (M_A + M_B)$ ) with atomic masses  $M_A$  and  $M_B$ , and  $m_e$  is the electron mass. The terms  $\Delta_{kl}^i$  are Born–Oppenheimer breakdown parameters, of which only the  $\Delta_{01}^i$  terms are significant. Equation (9) is thus essentially the same as Eq. (8), but with  $U_{01}/\mu(1 + (m_e/M_A)\Delta_{01}^A + (m_e/M_B)\Delta_{01}^B)$  replacing  $Y_{01}(1 + \epsilon/Y_{01} - 2P^2/Y_{01}(T_1 - T_0))$ . The  $\Delta_{01}$  terms may be expanded,<sup>2,3,8</sup>

$$\Delta_{01}^A = (\Delta_{01}^A)^{ad} + \frac{(\mu g_J)_B}{m_p} + \frac{\mu \Delta Y_{01}^{(D)}}{m_e B_e}, \quad (11)$$

where  $(\mu g_J)_B$  is the isotopically independent value of  $\mu g_J$  referred to nucleus  $B$  as the origin,<sup>2</sup>

$$(\mu g_J)_B = \mu g_J + 2c_A m_p M_A / (M_A + M_B) \quad (12)$$

and  $c_A$  is the formal charge on atom  $A$ ,  $\Delta Y_{01}^{(D)}$  is the Dunham correction. The mass of the proton is represented as  $m_p$ , and  $(\Delta_{01}^A)^{ad}$  represents the adiabatic contribution to  $\Delta_{01}^A$ . There is a corresponding expression for  $\Delta_{01}^B$ . The rotational  $g_J$  factor in a nonrelativistic approximation is given by<sup>32</sup>

$$g_J = \frac{m_p}{I_e} \left( \sum_i Z_i z_i^2 - \frac{2}{m_e} \sum_{k \neq 0} \frac{|\langle k | L_x | 0 \rangle|^2}{T_k - T_0} \right), \quad (13)$$

where  $Z_i$  and  $z_i$  are, respectively, the atomic number and position of atom  $i$ .  $L_x$  is an orbital angular momentum operator, and the sum over  $k$  is over all excited  $^1\Pi$  states.

When the terms of Eqs. (11), (12), and (13) are inserted into the expression for  $Y_{01}$  [Eq. (10)] and the result is simplified we obtain

TABLE II. Molecular constants in MHz for  $^{195}\text{Pt}^{32}\text{S}$  and  $^{195}\text{Pt}^{34}\text{S}$ .

Isotope	$v$	$B$	$10^3 D$	$(^{195}\text{Pt}) C_I$
$^{195}\text{Pt}^{32}\text{S}$	0	4412.370 43(99) <sup>a</sup>	1.440(136)	-0.066 80(157)
	1	4393.296 25(99)	1.429(136)	-0.065 63(157)
	2	4374.186 24(75)	1.429 <sup>b</sup>	-0.065 13(189)
$^{195}\text{Pt}^{34}\text{S}$	0	4190.141 26(75)	1.440 <sup>b</sup>	-0.064 53(189)
$^{195}\text{Pt}^{28}\text{Si}^c$	0	4851.219 96(99)	1.693(136)	+0.030 98(157)
$^{195}\text{PtCO}^d$	0	3322.833 56(31)	0.450(20)	+0.024 20(87)

<sup>a</sup>Numbers in parentheses are one standard deviation in units of the last significant figure.

<sup>b</sup>Constrained to this value.

<sup>c</sup>Reference 13.

<sup>d</sup>Reference 28.

$$Y_{01} = \frac{U_{01}}{\mu} \left[ 1 + \Delta_{01}^{ad} + \frac{\Delta Y_{01}^{(D)}}{B_e} + \frac{m_e}{I_e} \sum_i Z_i z_i^2 - \frac{2P_L^2}{Y_{01}(T_k - T_0)} \right], \quad (14)$$

where  $\Delta_{01}^{ad}$  is the total adiabatic correction to  $Y_{01}$ . In the final term,

$$P_L = \langle v, L, \Lambda = 1 | B_e \hat{L}_+ | v', L, \Lambda = 0 \rangle. \quad (15)$$

Also, it is assumed that only one excited  $^1\Pi$  electronic state contributes. In this term the distinction between  $B_e$ ,  $Y_{01}$ , and  $U_{01}/\mu$  is insignificant. If the adiabatic contribution and the small fourth term are ignored (or considered assimilated into the Dunham correction), and Eq. (14) is inserted into Eq. (9), then Eqs. (9) and (8) are found to be phenomenologically the same, albeit with  $P_L$  replacing  $P$ . However, in terms of angular momentum operators the  $L, \Lambda$  dependence of  $P_L$  is the same as the  $J_a, \Omega$  dependence of  $P$ . Accordingly Watson's formalism can be meaningfully used to fit  $0^+$  states in Hund's case (c).

The problem with Eq. (14) for spectral fitting is that all four correction terms are mass (isotope) dependent. It must be returned to the form in Eq. (10) which includes the mass-independent terms  $\Delta_{01}^A$  and  $\Delta_{01}^B$ . These are easily shown to become

$$\Delta_{01}^A = \left[ (\Delta_{01}^A)^{ad} + \frac{\mu \Delta Y_{01}^{(D)}}{m_e B_e} + \frac{2c_A M_A}{(M_A + M_B)} + \frac{\mu}{I_e} \sum_i Z_i z_i^2 - \frac{\mu}{m_e} \frac{2P_L^2}{Y_{01}(T_1 - T_0)} \right] \quad (16)$$

with a corresponding expression for  $\Delta_{01}^B$ . It will be noted that the term  $-\mu/m_e(2P_L^2/Y_{01}(T_1 - T_0))$  appears in the expressions for both  $\Delta_{01}^A$  and  $\Delta_{01}^B$ . If this term contributes much more than the others its effects will dominate both  $\Delta_{01}^A$  and  $\Delta_{01}^B$ .

While Eq. (10) is valid when the molecules contain light atoms alone, it must be modified when at least one of the atoms is heavy. In this case the nuclei can no longer be considered point charges: their charges are distributed over a finite volume to produce a so-called field-shift contribution. This can be accounted for by modifying Eq. (10) to<sup>8</sup>

$$Y_{01} = \frac{\bar{U}_{01}}{\mu} \left[ 1 + \frac{m_e}{M_A} \Delta_{01}^A + \frac{m_e}{M_B} \Delta_{01}^B + V_{01}^A \delta \langle r^2 \rangle_{AA'} + V_{01}^B \delta \langle r^2 \rangle_{BB'} \right], \quad (17)$$

where  $V_{01}^A$  and  $V_{01}^B$  are isotopically independent field-shift parameters as defined in Eq. (1). To apply Eq. (17) one isotopic species is chosen as a reference (e.g.,  $^{194}\text{Pt}^{32}\text{S}$ ), so that  $\delta \langle r^2 \rangle_{AA'}$  and  $\delta \langle r^2 \rangle_{BB'}$  are the changes in mean square nuclear charge radius on the isotopic substitutions  $A \rightarrow A'$  and  $B \rightarrow B'$ , respectively. The constant  $\bar{U}_{01}$  applies to the reference isotopic species. It is related to the mass-independent parameter  $U_{01}$  by

$$\bar{U}_{01} = U_{01} (1 + V_{01}^A \langle r^2 \rangle_A + V_{01}^B \langle r^2 \rangle_B). \quad (18)$$

in which  $\langle r^2 \rangle_A$  and  $\langle r^2 \rangle_B$  are mean-square charge radii of nuclei  $A$  and  $B$ , respectively, in the reference isotopic species.

The method of analysis of the spectrum of PtS was thus the following. An initial fit to the experimental data in Table I used Eqs. (9) and (10), including  $\Delta_{01}^{\text{Pt}}$  and  $\Delta_{01}^{\text{S}}$ , but ignoring possible field-shift effects. The other fitted constants were  $U_{01}$ ,  $U_{02}$ ,  $U_{11}$ , and  $U_{21}$ . The results are in Table III. In this table are given also values for the constants  $Y_{01}$ ,  $Y_{02}$ ,  $Y_{11}$ , and  $Y_{21}$  for each isotopomer. The r.m.s. deviation was 1.1 kHz, an entirely acceptable value in light of the measurement accuracies of the transition frequencies.

Several interesting features of the parameters in Table III are (a) the high precision of the fitted constants, especially  $U_{01}$  and  $U_{11}$ ; (b) the very large values of  $\Delta_{01}^{\text{Pt}}$  and  $\Delta_{01}^{\text{S}}$  and the fact that  $\Delta_{01}^{\text{S}} - \Delta_{01}^{\text{Pt}} \approx -20$ ; and (c) the isotopic variations of the  $r_e$  values calculated directly from the  $Y_{01}$  values. These variations are an order of magnitude bigger than those of many other molecules, of which PtSi is a good example.<sup>13</sup> Both the large  $\Delta_{01}$  values and these variations suggest that the limit of the Born–Oppenheimer approximation i.e., Born–Oppenheimer breakdown, BOE) is reached more easily than for many stable molecules.

To give some indication of the relative size of the  $\Delta_{01}$  terms, they are compared with those of other diatomic molecules studied to date in Table IV. With a few exceptions, both constants are an order of magnitude larger than those of all the other molecules. Given the case (c) coupling of PtS, it is likely that the interaction between close-lying  $1^+$  and  $0^+$  states is the cause of these large values.

The difference between  $\Delta_{01}^{\text{Pt}}$  and  $\Delta_{01}^{\text{S}}$  was now addressed. Values for the field-shift parameters  $V_{01}^{\text{Pt}}$  and  $V_{01}^{\text{S}}$  were estimated theoretically, as described in Sec. 2.2 above, and applied to Eq. (17). They were calculated to be  $-83.99 \times 10^{-7} \text{ fm}^{-2}$  and  $0.02 \times 10^{-7} \text{ fm}^{-2}$ , respectively. Clearly, only the term in  $V_{01}^{\text{Pt}}$  was significant. Values of  $\delta \langle r^2 \rangle_{\text{Pt}, \text{Pt}'}$  were obtained from tables.<sup>39</sup> The basis molecule was  $^{194}\text{Pt}^{32}\text{S}$ . It was found to have the correct sign and magnitude to account for the difference found in the  $\Delta_{01}$  values.

A new Dunham-type fit was then carried out using Eqs. (9) and (17). Because  $\Delta_{01}^{\text{Pt}}$  and  $V_{01}^{\text{Pt}}$  could not be separated with the experimental data alone, the fit instead assumed that  $\Delta_{01}^{\text{Pt}} = \Delta_{01}^{\text{S}} \pm 1$  (recall that Watson has shown that these two terms should be approximately, but not exactly, equal<sup>2</sup>); the values in Table IV indicate that this approximation is reasonable. The fit was thus to  $\bar{U}_{01}$ ,  $U_{02}$ ,  $U_{11}$ ,  $U_{21}$ ,  $\Delta_{01}^{\text{S}}$  and  $V_{01}^{\text{Pt}}$ , with  $V_{01}^{\text{S}}$  set to zero. The resulting values of  $\bar{U}_{01}$ ,  $\Delta_{01}^{\text{S}}$ , and  $V_{01}^{\text{Pt}}$  are given in Table IV. The remaining terms ( $U_{02}$ ,  $U_{11}$ , and  $U_{21}$ ) were found to agree with the values given in Table III within the experimental uncertainties. The agreement between  $V_{01}^{\text{Pt}}$  determined in this way and using DFT is very good.

## IV. DISCUSSION

### A. Internuclear distance

Enough data have been obtained to evaluate the equilibrium internuclear distance  $r_e$  of PtS. This can be done using

TABLE III. Mass-independent and -dependent Dunham parameters for nine isotopomers of PtS.

	$U_{01}$ (uMHz)	$U_{02}$ (u <sup>2</sup> MHz)	$U_{11}$ (u <sup>3/2</sup> MHz)	$U_{21}$ (u <sup>2</sup> MHz)	$\Delta_{01}^{\text{Pt}}$	$\Delta_{01}^{\text{S}}$
PtS	121 604.07(30) <sup>a</sup>	-1.092(3)	-2740.693(47)	-13.48(8)	-42.69(74)	-62.47(5)
Parameter <sup>d</sup>	$Y_{01}$ (MHz) <sup>b</sup> $B_e$	$10^3 Y_{02}$ (MHz) $-10^3 D_e$	$Y_{11}$ (MHz) $-\alpha_e$	$10^3 Y_{21}$ (MHz) $10^3 \gamma_e$	$r_e$ (Å) <sup>c</sup>	
<sup>194</sup> Pt <sup>32</sup> S	4425.109 88	-1.449	-19.059 06	-17.89	2.039 828 30	
<sup>195</sup> Pt <sup>32</sup> S	4421.893 99	-1.447	-19.038 27	-17.87	2.039 827 71	
<sup>196</sup> Pt <sup>32</sup> S	4418.717 15	-1.445	-19.017 74	-17.84	2.039 827 05	
<sup>198</sup> Pt <sup>32</sup> S	4412.451 64	-1.441	-18.977 27	-17.79	2.039 825 82	
<sup>192</sup> Pt <sup>32</sup> S	4431.633 44	-1.454	-19.101 26	-17.95	2.039 829 69	
<sup>194</sup> Pt <sup>34</sup> S	4202.168 71	-1.307	-17.635 37	-16.13	2.039 763 90	
<sup>195</sup> Pt <sup>34</sup> S	4198.952 48	-1.305	-17.615 11	-16.11	2.039 763 30	
<sup>196</sup> Pt <sup>34</sup> S	4195.775 30	-1.303	-17.595 10	-17.60	2.039 762 67	
Covariances from least squares fit <sup>e</sup>						
$U_{01}$	1					
$U_{02}$	0.000	1				
$U_{11}$	-0.001	0.000	1			
$U_{21}$	0.003	0.000	-0.003	1		
$\Delta_{01}^{\text{Pt}}$	-0.208	0.000	0.004	-0.010	1	
$\Delta_{01}^{\text{S}}$	-0.008	0.000	0.000	0.000	0.010	1

<sup>a</sup>Numbers in parentheses are one standard deviation in units of the last significant figure.

<sup>b</sup>The mass-dependent Dunham parameters  $Y_{kl}$  have been obtained from the mass-independent parameters,  $U_{kl}$ , by Eq. (10).

<sup>c</sup>Calculated from  $Y_{01}$  using  $Y_{01} = h/8\pi^2 \mu r_e^2$ , where  $\mu$  is the atomic reduced mass.

<sup>d</sup>Spectroscopic parameters to which  $Y_{kl}$  is approximately equal, where  $E_{v,J} = J(J+1)[B_e - D_e J(J+1) - \alpha_e(v + 1/2) + \gamma_e(v + 1/2)^2 - \epsilon_e(v + 1/2)^3]$ .

<sup>e</sup>r.m.s.=1.95 kHz; no. of data points=33; no. of isotopomers=8.

several methods, which each give slightly different results, and considerable care must be taken in their interpretation.

The first method used the  $Y_{01}$  values for each isotopomer in the equation,<sup>40</sup>

$$r_e = \frac{C_2}{\sqrt{Y_{01}(\text{MHz})\mu(u)}}, \quad (19)$$

where  $\mu$  is the reduced mass of the isotopomer, and

$$C_2 = \sqrt{\frac{10^{17} h N_A}{8 \pi^2}} = 710.900 137 9(25) \text{ \AA MHz}^{-1/2} u^{-1/2}. \quad (20)$$

$C_2$  has been evaluated using the fundamental constants recommended by CODATA in 1998 in the paper by Mohr and Taylor.<sup>41</sup> The values for each isotopomer, which are in Table III, were obtained using the 1993 atomic masses published by Audi and Wapstra.<sup>42</sup> There is a variation with isotopomer over  $6 \times 10^{-5}$  Å, which is nearly two orders of magnitude bigger than the uncertainties, indicating clearly the onset of Born–Oppenheimer breakdown at this point. It is also an order of magnitude bigger than the corresponding variation in PtSi,<sup>13</sup> though the variation found in ZnO (Ref. 10) is comparable.

The parameter  $\bar{U}_{01}$ , obtained in the fit including Pt nuclear field-shift effects, which is given in Table IV, was used to obtain  $r_e^v$ . This is an equilibrium distance in which volume effects are included, and was determined with<sup>4</sup>

$$r_e^v = \sqrt{\frac{h}{8 \pi^2 \bar{U}_{01}}}. \quad (21)$$

The result, which is given in Table V, applies to the reference isotopomer, <sup>194</sup>Pt<sup>32</sup>S.

The isotopically independent Born–Oppenheimer bond length  $r_e^{\text{BO}}$ , in which field-shift effects have been accounted for, was obtained using  $U_{01}$  from  $\bar{U}_{01}$  in Eq. (17). For this purpose the value  $V_{\text{Pt}}$  from Table IV was used, with  $\langle r^2 \rangle_{\text{Pt}}$  for <sup>195</sup>Pt as 28.90(10) fm<sup>2</sup> from Ref. 44. Although  $\langle r^2 \rangle_{\text{S}}$  is unknown, it is undoubtedly smaller than  $\langle r^2 \rangle_{\text{Pt}}$ ; given that in addition  $V_{\text{S}}$  is calculated to be  $0.02 \times 10^{-7}$  fm<sup>-2</sup>, i.e., three orders of magnitude smaller than  $V_{01}^{\text{Pt}}$ , the term  $V_{\text{S}} \langle r^2 \rangle_{\text{S}}$  was ignored. The resulting value of  $U_{01}$  is in Table IV. A value for  $r_e^{\text{BO}}$  was then calculated using Eq. (20) with  $\bar{U}_{01}$  replaced by  $U_{01}$ ; it is given in Table V. Its uncertainty is set by the assumed uncertainty in  $\Delta_{01}^{\text{Pt}}$ , which ultimately affects that of  $U_{01}$ .

The analysis started with the assumption that if the  $\Delta_{01}$  values were small enough then the formalism of  $X^1\Sigma^+$  molecules would apply, and the  $Y_{kl}(U_{kl})$  constants would have clear physical interpretation. This is the basis on which the  $r_e$  values were calculated. It should thus be expected that they should agree well with the *ab initio* values. The comparison in Table V shows that this is indeed the case.

TABLE IV. Watson-type  $\Delta_{01}$  terms, field-shift terms  $V_A$  (where known), and mass reduced Dunham-type coefficient  $U_{01}$  for several diatomic molecules.

$AB$	$\Delta_{01}^A$	$\Delta_{01}^B$	$10^{-7}V_{01}^A(\text{fm}^{-2})$	$U_{01}(\mu\text{MHz})$	Reference
PtS	-42.60(74) <sup>a</sup>	-62.466(49)		121 604.07(30) <sup>b</sup>	This work
	-62.5(10) <sup>c</sup>	-62.46(5)	-104(9)	$\bar{U}_{01}=121\ 610.91(50)$ $U_{01}=121\ 647.1(20)^d$	
			-84 <sup>e</sup>		
PtSi	10.75(68)	-2.99(4)		118 923.32(33) <sup>b</sup>	13
	-3(1) <sup>c</sup>	-2.99(4)	-72(12)	$\bar{U}_{01}=118\ 927.94(54)$ $U_{01}=118\ 952.7(47)^d$	
			-110 <sup>e</sup>		
BiN	...	-2.788(19)		135 003.18(10) <sup>b</sup>	14
	-2.8(10) <sup>c</sup>	-2.788(19)	32 <sup>e</sup>	$\bar{U}_{01}=135\ 004.17(10)$ $U_{01}=134\ 991.08(45)^d$	
ZrO	-4.872(39)	-6.1888(25)		172 480.086(98)	10
ZrS	-5.325(82)	-6.523(39)		108 670.07(19)	10
HfO	-3.40(57)	-5.656(23)		170 239.68(18) <sup>f</sup>	11
HfS	-4.18(53)	-5.820(49)		108 708.38(27)	12
AlCl <sup>g</sup>	...	-1.4427(287)		111 378.117(49)	33
InF <sup>h</sup>	...	...		128 210.086(10)	34
GeSe	-1.505(87) <sup>i</sup>	-1.86(14) <sup>i</sup>		110 913.1(82)	35
GaH	-2.62(35)	-4.2181(13)		183 363.95(42)	36
CO	-2.0545(12)	-2.0982(13)		397 029.003(24)	37
ClH	-0.26(20)	0.1262(8)		311 077.90(96)	38
PbS	-12.94(141)	-1.997(71)		96 642.20(50) <sup>f</sup>	7
PbS <sup>j</sup>	-1.333 <sup>k</sup>	-1.988(70)	26.38(51)		9
TlCl	-18.96(200)	-1.243(49)		81857.0(1) <sup>f</sup>	7
TlCl <sup>l</sup>	-0.500 <sup>k</sup>	-1.257(73)	40.9(55)		9

<sup>a</sup>The numbers in parentheses are one standard deviation in units of the last significant figure.

<sup>b</sup>In this fit field-shift effects were neglected.

<sup>c</sup>This is an estimated value and uncertainty based on the assumption that  $\Delta_{01}^A = \Delta_{01}^B \pm 1$ . This allows field-shift effects to be considered in the fitting procedure, see text for details.

<sup>d</sup>Value calculated from  $\bar{U}_{01}$  using Eq. (18); see text.

<sup>e</sup>This value was obtained using DFT following the methods outlined in Ref. 15. In the case of BiN,<sup>14</sup> the calculated value was used in the determination of  $\bar{U}_{01}$  and  $U_{01}$ .

<sup>f</sup>This value for  $U_{01}$  has been calculated from the data given in the appropriate reference.

<sup>g</sup>Because of the occurrence of only one naturally occurring isotope of Al only  $\Delta_{01}^{\text{Cl}}$  terms could be determined.

<sup>h</sup> $\Delta_{01}^i$  terms were not determined.

<sup>i</sup>These numbers are actually  $\Delta^B$  terms determined from a fit to Dunham potential parameters, but differ from  $\Delta_{01}^B$  terms only in that they do not contain a contribution from the Dunham correction, which is expected to be small.

<sup>j</sup>In this fit allowance was made for nuclear field-shift effects resulting in a reduction in magnitude for the  $\Delta_{01}^A$  terms.

<sup>k</sup>This value was held fixed during this fitting procedure, Ref. 8 should be consulted for the specific details of the fitting procedure used.

TABLE V. Internuclear distances of PtS and related compounds.

Molecule	Bond length ( $\text{\AA}$ )	Remarks (Ref.)
PtS ( $X^0+$ )	$r_e = 2.039\ 828\ 30(70)^{a,b}$	Expt. (this work)
	$r_e^v = 2.038\ 553(4)^b$	Expt. (this work)
	$r_e^{\text{BO}} = 2.038\ 250(13)$	Expt. (this work)
	$r_e = 2.0376$	DFT calculation (this work)
	SAOP+HCTH(93)/QZ4P (Ref. 43)	
PtSi ( $X^1\Sigma^+$ )	$r_e^{\text{BO}} = 2.061\ 206(42)$	Expt. (Ref. 13)
PtC ( $X^1\Sigma^+$ )	$r_e = 1.679$	Expt. (Ref. 19)
PtN ( $X^2\Pi$ )	$r_e = 1.682$	Expt. (Ref. 19)
PtO ( $X^3\Sigma^-$ )	$r_e = 1.727$	Expt. (Ref. 19)

<sup>a</sup>Numbers in parentheses are one standard deviation in units of the last significant figure.

<sup>b</sup>Value obtained for the reference isotopomer  $^{194}\text{Pt}^{32}\text{S}$ .

## B. General topics

Kratzer<sup>45</sup> and Pekeris<sup>46</sup> have presented equations whereby the vibration frequency, anharmonicity constant, and dissociation energy of a diatomic molecule can be estimated. These are

$$Y_{10} \approx \omega_e \approx \sqrt{\frac{4Y_{01}^3}{-Y_{02}}}, \quad (22)$$

$$Y_{20} \approx \omega_e x_e \approx Y_{01} \left( \frac{-Y_{11}Y_{10}}{6Y_{01}^2} + 1 \right)^2, \quad (23)$$

TABLE VI. Estimated and DFT calculated spectroscopic parameters for  $^{194}\text{Pt}^{32}\text{S}$ .

Parameter	Value	Remarks (Ref.)
$\omega_e$	511(5) $\text{cm}^{-1\text{a}}$	This work using Eq. (22)
	532.1 $\text{cm}^{-1}$	This work, DFT calc. <sup>b</sup>
	549.45 $\text{cm}^{-1}$	Ref. 16
$\omega_e x_e$	1.79(3) $\text{cm}^{-1}$	This work using Eq. (23)
	2.75 $\text{cm}^{-1}$	This work, DFT calc. <sup>b</sup>
$\alpha_e$	0.000 635 7(1) $\text{cm}^{-1}$	This work
	0.000 69 $\text{cm}^{-1}$	This work, DFT calc. <sup>b</sup>
$D_e$	407(11) $\text{kJ mol}^{-1}$	This work using Eq. (24)
	468 $\text{kJ mol}^{-1}$	This work, DFT calc. <sup>b</sup>

<sup>a</sup>Numbers in parentheses are one standard deviation error in units of the last significant figure.

<sup>b</sup>This result has been obtained using a potential energy curve for PtS prepared using the SAOP+HCTH(93)/QZ4P (Ref. 43) method. Spectroscopic constants were then obtained from the potential energy curve using Dunning's VIBROT program (Ref. 47).

$$D_e \approx \frac{Y_{10}^2}{4Y_{20}}. \quad (24)$$

The values for  $^{194}\text{Pt}^{32}\text{S}$  have been estimated from its  $Y_{kl}$  constants in Table III and are given together with the spectroscopic constants obtained from the DFT potential energy curve in Table VI. The agreement between  $\omega_e$  obtained using Eq. (22) and the value obtained using isotope shifts in Ref. 16 is poor; the value obtained from the DFT calculation is intermediate between the two numbers.

It is clear from Tables IV and V that the values of  $\Delta_{01}^{\text{Pt}}$  and  $\Delta_{01}^{\text{S}}$  are unusually large. It is not unreasonable that the cause is a low-lying  $1^+$  excited state. A brief inspection of Eqs. (14) and (10) shows that

$$\frac{m_e}{M_{\text{Pt}}} \Delta_{01}^{\text{Pt}} + \frac{m_e}{M_{\text{S}}} \Delta_{01}^{\text{S}} \approx -\frac{2P_L^2}{Y_{01}(T_1 - T_0)} \equiv -\frac{2P^2}{Y_{01}(T_1 - T_0)}. \quad (25)$$

If we assume  $\Delta_{01}^{\text{Pt}} = \Delta_{01}^{\text{S}} = -62.5$  (as in Table V), the spin-orbit energy gap  $1^+ - 0^+ [\equiv (T_1 - T_0)]$  can in principle be estimated. However, the value of  $P$  is a problem: In the idealized “pure precession” approximation it is given roughly by<sup>29,31</sup>

$$P \sim B \sqrt{J_a(J_a + 1)}, \quad (26)$$

but the value of  $J_a$  is unknown. For Bi (Ref. 31) it was assumed that  $J_a = 1$  is reasonable, making  $P = B\sqrt{2}$ . For PtS this approximation gives  $(T_1 - T_0) \sim 471 \text{ cm}^{-1}$ . This value is not far from  $\omega_e$  (Table VI). However, there were no hints of perturbations in the spectra of vibrationally excited molecules. In addition, there is no mention of a low-lying excited electronic state in the literature. Furthermore,  $(T_1 - T_0) \sim 471 \text{ cm}^{-1}$  seems low. We may make a comparison to the related molecule PtO, for which  $(T_1 - T_0)$  is reported from its electronic spectrum as  $946 \text{ cm}^{-1}$ .<sup>17</sup> From its microwave spectrum we have recently<sup>48</sup> obtained, assuming  $P = B\sqrt{2}$  a value of  $\sim 612 \text{ cm}^{-1}$ , which is significantly lower. Evidently the approximation that  $J_a = 1$  is poor for PtO; this is likely also the case for PtS. Given that the unpaired electrons are in  $\pi$ -molecular orbitals with a significant contribution from  $5d$  on Pt ( $l = 2!$ ) (see below), this is perhaps un-

surprising. On the other hand, our results do suggest that  $(T_1 - T_0)$  decreases on going from PtO to PtS. Although this trend is not intuitive, a similar result has been observed for the Bi-monohalides, where  $(T_1 - T_0)$  decreases in the order  $\text{BiF} > \text{BiCl} > \text{BiBr} > \text{BiI}$ .<sup>49</sup>

Table II shows that the nuclear spin-rotation constant,  $C_I(^{195}\text{Pt})$  is large, and of opposite sign compared to those found for PtSi and PtCO. In the case of  $X^1\Sigma$  molecules negative values for  $C_I$  are unusual<sup>50</sup> (see also, for example, Ref. 51). It was thus reasonable to anticipate that this value has arisen in PtS because of the case (c) coupling. To our knowledge  $C_I$  values for only two comparable molecules have been measured. These are BiF (Ref. 52) and BiCl (Ref. 53). Both have  $X0^+$  ground electronic states, and in both cases  $C_I(\text{Bi})$  is negative. For BiF and BiCl, Tischer, Müller, and Törring<sup>50</sup> rationalized the negative  $C_I(\text{Bi})$  constants in the bismuth halides in the following way. Initially the microscopic hyperfine structure Hamiltonian for a  $^3\Sigma$  state taken from Frosch and Foley<sup>54</sup> was used to derive an expression for the effective nuclear spin-rotation constant,  $(C_I)_{\text{eff}}$ . The constant  $(C_I)_{\text{eff}}$  is the experimental nuclear spin-rotation constant obtained from the frequency measurements using a hyperfine structure energy formula, generally applicable to a  $^1\Sigma$ -state molecule (as has been done here). The expression obtained by Tischer, Müller, and Törring,<sup>50</sup> is

$$(C_I)_{\text{eff}} = f + (b - f) \sin \chi_J / [J(J + 1)]^{1/2} + (b + c - f) \sin^2 \frac{1}{2} \chi_J / J(J + 1), \quad (27)$$

where  $f$  is the nuclear spin-rotation interaction constant, the angle  $\chi_J$  is the angle representing the unitary transformation required to diagonalize the energy matrix for a molecule with a ground state  $\Omega = 0^+$  which is coupled by a weak Coriolis interaction to the  $1^+$  state. This angle may be approximated by

$$\tan \chi_J \approx 2\sqrt{2} \frac{P}{T_1 - T_0} [J(J + 1)]^{1/2}. \quad (28)$$

To a good approximation the remaining constants in Eq. (27) are<sup>55</sup>

$$b = g_N \mu_B \mu_N \left[ \frac{16\pi}{3} |\psi(0)|^2 - \left( \frac{3 \cos^2 \theta - 1}{r^3} \right)_{\text{av}} \right] \quad (29)$$

$$c = 3 g_N \mu_B \mu_N \left( \frac{3 \cos^2 \theta - 1}{r^3} \right)_{\text{av}} \quad (30)$$

$|\psi(0)|^2$  is the probability of finding unpaired electron density at the nucleus in question,  $g_N$  is its nuclear  $g$  factor,  $\mu_B$  and  $\mu_N$  are the Bohr and nuclear magnetons, respectively,  $r$  is the distance between the nucleus and electron, and  $\theta$  is the angle between the internuclear axis and the radius vector from nucleus to electron.

Tischer *et al.* show that owing to a small rotation angle  $\chi_J$  in the case of the Bi-halides the terms in Eq. (27) involving  $\sin^2(1/2)\chi_J/J(J+1)$  may be neglected. The negative sign of  $(C_I)_{\text{eff}}(\text{Bi})$  is therefore shown to arise in Eq. (27) from a large and negative rotational hyperfine structure constant  $b$ .

A very similar situation applies for PtS. Its  $T_1 - T_0$  gap has been estimated in the BOB analysis given above to be smaller than the corresponding gap for the Bi halides. However, since only low  $J$  transitions have been observed for PtS, Eq. (28) shows that  $\chi_J$  is small,  $\approx 0.1^\circ$  for the highest  $J$  observed ( $J=2$ ). Accordingly the ground state is nearly a pure  $X0^+$  state, and the terms in Eq. (27) involving  $\sin^2(1/2)\chi_J/J(J+1)$  may again be neglected. Just as with the Bi halides, a negative  $C_I(^{195}\text{Pt})$  requires  $b$  also to be negative. Population analysis from our DFT calculation shows that the unpaired electrons in PtS (which are in a  $\pi$  orbital) have contributions of  $\approx 0.63p$  from S and  $\approx 0.45d$  from Pt. The lack of  $s$ -atomic character from Pt makes  $|\psi(0)|^2$  in Eq. (26) essentially zero, so that  $b$  is again negative because of the  $((3 \cos^2 \theta - 1)/r^3)_{\text{av}}$  term.

A crude estimate for  $f$  might be the value of  $C_I(^{195}\text{Pt}) \approx 30$  kHz, recently found for  $^{195}\text{PtSi}$ .<sup>13</sup> This would permit a similarly crude estimate of  $b[\approx -g_N\mu_B\mu_N((3 \cos^2 \theta - 1)/r^3)_{\text{av}}]$  of the order of  $-20$  MHz. Such a value is not unreasonable.

## V. CONCLUSIONS

The pure rotational spectrum of PtS in its ground electronic state has been measured using a cavity pulsed jet Fourier-transform microwave spectrometer. Though the molecule has two unpaired electrons suggesting a triplet ground state, it actually obeys Hund's case (c), and the observed state was  $X0^+$ . As a result the spectrum could be analyzed using the formalism normally used for closed shell  $1\Sigma^+$  states. This procedure has been shown to be valid. The Born–Oppenheimer breakdown parameters  $\Delta_{01}^{\text{Pt}}$  and  $\Delta_{01}^{\text{S}}$  have been shown to be large and negative because of a low-lying  $1^+$  state. The difference between  $\Delta_{01}^{\text{Pt}}$  and  $\Delta_{01}^{\text{S}}$  has been shown to be dominated by nuclear field-shift effects at Pt. A large negative Pt nuclear spin-rotation constant  $C_I(^{195}\text{Pt})$  has been rationalized in terms of the dipole-dipole electron-nucleus hyperfine coupling constant  $b$ . The equilibrium bond length  $r_e$  has been evaluated, along with the vibration frequency and dissociation energy.

## ACKNOWLEDGMENTS

This research has been supported by the Natural Sciences and Engineering Research Council (NSERC) of Canada and by the Petroleum Research Fund, administered by the American Chemical Society.

<sup>1</sup>J. L. Dunham, Phys. Rev. **41**, 721 (1932).

<sup>2</sup>J. K. G. Watson, J. Mol. Spectrosc. **45**, 99 (1973).

<sup>3</sup>J. K. G. Watson, J. Mol. Spectrosc. **80**, 411 (1980).

<sup>4</sup>P. R. Bunker, J. Mol. Spectrosc. **35**, 307 (1970).

<sup>5</sup>P. R. Bunker, J. Mol. Spectrosc. **68**, 367 (1977).

<sup>6</sup>R. J. LeRoy, Chemical Physics Research Report No. CP-633, University of Waterloo, Ontario, 1998.

<sup>7</sup>E. Tiemann, H. Arnst, W. U. Steida, T. Törring, and J. Hoefl, Chem. Phys. **67**, 133 (1982).

<sup>8</sup>J. Schlembach and E. Tiemann, Chem. Phys. **68**, 21 (1982).

<sup>9</sup>H. Knöckel, T. Kröckertskoth, and E. Tiemann, Chem. Phys. **93**, 349 (1985).

<sup>10</sup>S. A. Beaton and M. C. L. Gerry, J. Chem. Phys. **110**, 10715 (1999).

<sup>11</sup>A. Lessari, D. J. Brugh, and R. D. Suenram, J. Chem. Phys. **117**, 9651 (2002).

<sup>12</sup>S. A. Cooke and M. C. L. Gerry, J. Mol. Spectrosc. **216**, 122 (2002).

<sup>13</sup>S. A. Cooke, M. C. L. Gerry, D. J. Brugh, and R. D. Suenram, J. Mol. Spectrosc. **223**, 185 (2004).

<sup>14</sup>S. A. Cooke, J. M. Michaud, and M. C. L. Gerry, J. Mol. Struct. **695–696**, 13 (2004).

<sup>15</sup>S. A. Cooke, M. C. L. Gerry, and D. P. Chong, Chem. Phys. **298**, 205 (2004).

<sup>16</sup>B. Z. Li, K. Y. Jung, and T. C. Steimle, J. Mol. Spectrosc. **170**, 310 (1995).

<sup>17</sup>U. Sassenberg and R. Scullman, Phys. Scr. **28**, 139 (1983).

<sup>18</sup>C. I. Frum, R. Engelman, and P. F. Bernath, J. Mol. Spectrosc. **150**, 566 (1991).

<sup>19</sup>T. C. Steimle, K. Y. Jung, and B. Z. Li, J. Chem. Phys. **103**, 1767 (1995).

<sup>20</sup>K. A. Walker and M. C. L. Gerry, J. Mol. Spectrosc. **182**, 178 (1997).

<sup>21</sup>T. J. Balle and W. H. Flygare, Rev. Sci. Instrum. **52**, 33 (1981).

<sup>22</sup>Y. Xu, W. Jäger, and M. C. L. Gerry, J. Mol. Spectrosc. **151**, 206 (1992).

<sup>23</sup>SCM, *ADF Program System, Release 2002.03* (Scientific Computing and Modelling NV, Amsterdam, 2000), see www.scm.com

<sup>24</sup>E. van Lenthe, E. J. Baerends, and S. G. Snijders, J. Chem. Phys. **101**, 9783 (1994).

<sup>25</sup>E. van Lenthe, A. E. Ehlers, and E. J. Baerends, J. Chem. Phys. **110**, 8943 (1999).

<sup>26</sup>P. R. T. Schipper, O. V. Gritsenko, S. J. A. van Gisbergen, and E. J. Baerends, J. Chem. Phys. **112**, 1344 (2000).

<sup>27</sup>H. M. Pickett, J. Mol. Spectrosc. **148**, 371 (1991).

<sup>28</sup>C. J. Evans and M. C. L. Gerry, J. Phys. Chem. A **105**, 9659 (2001).

<sup>29</sup>L. Veseth, J. Phys. B **6**, 1473 (1973).

<sup>30</sup>L. Veseth, J. Phys. B **6**, 1484 (1973).

<sup>31</sup>P. Kuijpers, T. Törring, and A. Dymanus, Chem. Phys. **12**, 309 (1976).

<sup>32</sup>W. Gordy and R. L. Cook, *Microwave Molecular Spectra: Techniques in Chemistry* (Wiley, New York, 1984), Vol. 18.

<sup>33</sup>H. Hedderich, M. Dulick, and P. F. Bernath, J. Chem. Phys. **99**, 8363 (1993).

<sup>34</sup>T. Karkanis, M. Dulick, Z. Morbi, J. B. White, and P. F. Bernath, Can. J. Phys. **72**, 1213 (1994).

<sup>35</sup>T. Konno and H. Uehara, Chem. Phys. Lett. **247**, 529 (1995).

<sup>36</sup>J. M. Campbell, M. Dulick, D. Klapstein, J. B. White, and P. F. Bernath, J. Chem. Phys. **99**, 8379 (1993).

<sup>37</sup>N. Authier, N. Bagland, and A. L. Floch, J. Mol. Spectrosc. **160**, 590 (1993).

<sup>38</sup>G. Guelachvili, P. Niay, and P. Bernage, J. Mol. Spectrosc. **85**, 271 (1981).

<sup>39</sup>P. Aufmuth, K. Helig, and A. Steudel, At. Data Nucl. Data Tables **37**, 455 (1987).

<sup>40</sup>C. S. Dickinson, J. A. Coxon, N. R. Walker, and M. C. L. Gerry, J. Chem. Phys. **115**, 6979 (2001).

<sup>41</sup>P. J. Mohr and B. N. Taylor, Rev. Mod. Phys. **72**, 351 (2000).

<sup>42</sup>G. Audi and A. H. Wapstra, Nucl. Phys. A **565**, 1 (1993).

<sup>43</sup>F. A. Hamprecht, A. J. Cohen, D. J. Tozer, and N. C. Handy, J. Chem. Phys. **109**, 6264 (1998).

<sup>44</sup>E. D. Nadjakov, K. P. Marinova, and Y. P. Gangrsky, At. Data Nucl. Data Tables **56**, 133 (1994).

<sup>45</sup>A. Kratzer, Z. Phys. **3**, 289 (1920).

<sup>46</sup>C. L. Pekeris, Phys. Rev. **45**, 98 (1934).

<sup>47</sup>T. H. Dunning, Jr. (private communication).

<sup>48</sup>S. A. Cooke and M. C. L. Gerry (unpublished).

<sup>49</sup>M. Beutel, K. D. Setzer, O. Shestakov, and E. H. Fink, J. Mol. Spectrosc. **175**, 48 (1996).

<sup>50</sup>R. Tischer, K. Möller, and T. Törring, Chem. Phys. **62**, 115 (1981).

<sup>51</sup>H. S. P. Müller and M. C. L. Gerry, J. Chem. Phys. **103**, 577 (1995).

<sup>52</sup>P. Kuijpers and A. Dymanus, Chem. Phys. **24**, 97 (1977).

<sup>53</sup>P. Kuijpers, T. Törring, and A. Dymanus, Chem. Phys. **18**, 401 (1976).

<sup>54</sup>R. A. Frosch and H. M. Foley, Phys. Rev. **88**, 1337 (1952).

<sup>55</sup>S. L. Miller and C. H. Townes, Phys. Rev. **90**, 537 (1953).